DOI: 10.1002/ejic.201100605

The Zinc-Dependent Fluorescence of a Synthetic GFP-Like Chromophore in Organic Solvents

Juntao Kang,[a] Xinxiu Fang,[a] Xiankai Chen,[b] Guiyan Zhao,[a] Aimin Ren,[b] Jingwei Xu,*[a] and Wei Yang*[a]

Keywords: Luminescence / Sensors / Fluorescent sensors / Zinc / Green fluorescent protein analogue / Chromophores / Density functional calculations / Solvent effects

A synthetic green fluorescent protein analogue showed Zn^{2+}-induced fluorescence in organic solvents (Φ = 0.07 at r.t. and up to 0.3 at low temperature). The experimental observations and theoretical calculations suggest that Zn^{2+} binding inhibits the free rotation of an aryl–alkene bond, which allows excited molecules to relax through the emission pathway instead of the thermodynamic pathway. The solvent influenced the fluorescence intensities and wavelengths by direct or indirect interactions with the molecules.

Introduction

Zinc is the second-most abundant metal ion in the human body. Cellular Zn^{2+} varies from the nanomolar range to about 0.3 mM.[1,2] It plays diverse roles in multiple biological processes.[3–8] A disorder of the Zn^{2+} metabolism is closely associated with many severe neurological diseases.[9,10]

Unlike other biological transition metal ions, Zn^{2+} does not give any spectroscopic or magnetic signals due to its $3d^{10}4s^0$ electronic configuration.[1,3,11] Fluorescence stands out as a suitable method for real-time and real-space imaging of Zn^{2+} without cell damage. Although many fluorescent indicators for Zn^{2+} have been designed and synthesized, none can perfectly satisfy all the requirements (see refs.[1,2] for the requirements for Zn^{2+} indicators). Thus, efforts to design new Zn^{2+} probes should be encouraged.[12,13]

Green fluorescent protein (GFP) has been widely applied to living cell labeling.[14,15] The advanced fluorescent properties of its chromophore have enabled researchers to develop cation sensors.[16] Synthetic GFP analogues are valuable as they can be applied in various environments, which include those that will unfold the protein.[17–20] In recent decades, great efforts have been devoted to developing cation sensors based on GFP analogues but the desired products are yet to be achieved.

The natural GFP chromophore is formed by the cyclization of a Ser–Tyr–Gly tripeptide in a deeply buried environment.[21] The π-conjugated system of the fluorescent chromophore consists of a phenol group and an imidazole ring that are linked by an aryl–alkene bond.[22,23] The isolated chromophores, and most synthetic analogues, possess very weak fluorescence due to the free rotation about the aryl–alkene bond.[24,25] In GFPs, this free rotation is inhibited by the tightly packed protein structure. For isolated molecules, chemical modification has been used to fix the configuration of the molecule.[19] We have previously shown that a hydrogen bond is sufficient to prohibit free rotation of the bond.[26] Similarly, ionic bonds formed by Zn^{2+} and two ligands located on the two rings are capable of inhibiting the free rotation about the aryl–alkene bond, which allows the molecule to emit in the presence of Zn^{2+} in solution.[27–29]

Results and Discussion

Zn^{2+}-Related Fluorescence

To mimic the chromophore of GFP, we synthesized 4-[(5*Z*)-{5-oxo-2-phenyloxazol-4(5*H*)-ylidene}methyl]-1*H*-imidazole-1-carboxylate (OPMIC) (Figure 1) and investigated its Zn^{2+}-dependent properties. The synthetic process was initiated from Boc-protected imidazole-4-carboxaldehyde, which reacted with hippuric acid at 75 °C to give Boc-protected OPMIC (Boc-OPMIC). The Boc-group was removed in the presence of trifluoroacetic acid (TFA). The Zn^{2+}-binding ability of the molecules was confirmed by UV/Vis and NMR spectroscopic studies (see Figures S1 and S2 in the Supporting Information).

[a] The State Key Laboratory of Electroanalytic Chemistry, Changchun Institute of Applied Chemistry, Changchun, Jilin 130022, China
Fax: +86-431-8526-2349
E-mail: yangwei@ciac.jl.cn
jwxu@ciac.jl.cn
[b] State Key Laboratory of Theoretical and Computational Chemistry, Institute of Theoretical Chemistry, Jilin University, Changchun, Jilin 130023, China

Supporting information for this article is available on the WWW under http://dx.doi.org/10.1002/ejic.201100605.

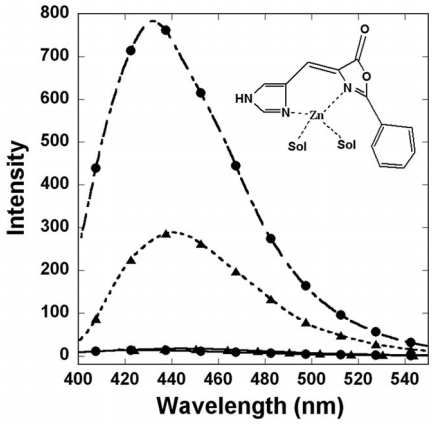

Figure 1. The fluorescence emission spectra of ca. 20 μM solutions of OPMIC (▲) and Boc-OPMIC (●) with (dashed lines) and without (solid lines) Zn^{2+} (1 mM) in acetone. Inset: OPMIC and its predicted binding mode to Zn^{2+}.

As predicted, both OPMIC and Boc-OPMIC interact with Zn^{2+} and exhibit Zn^{2+}-related fluorescence (Figures 1, and Figures S3–S4). In addition to Zn^{2+}, only Fe^{3+} induced strong fluorescence (Figure 2), whereas other cations did not cause obvious emissions. Further competition experiments showed that transition metal cations, especially Cu^{2+}, Co^{2+}, Cr^{3+}, and La^{3+}, greatly suppressed Zn^{2+}-induced fluorescence (Figure S5), which suggests that these cations also interacted with the molecules. Thus, the different fluorescent behavior of these metal ions is due to other mechanisms, possibly involving the quenching effects of these heavy metal cations. The competition of Fe^{3+} with Zn^{2+} did not reduce the fluorescence because both Fe^{3+} and Zn^{2+} induced the molecules to emit.

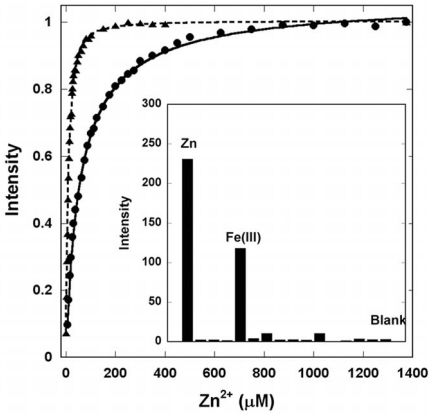

Figure 2. The fluorescence signals of OPMIC (▲) and Boc-OPMIC (●) as a function of Zn^{2+} in dixoane. The lines were generated by fitting the data with Hill's equation.[31] Inset: histogram showing flourescence intensity of Boc-OPMIC with added cations (from left to right: Zn^{2+}, Pb^{2+}, Mn^{2+}, Fe^{2+}, Fe^{3+}, Hg^{2+}, Cd^{2+}, Mg^{2+}, K^{+}, Ca^{2+}, Al^{3+}, Cu^{2+}, Co^{2+}, Cr^{3+}, and La^{3+}. The bar at the far right is Boc-OPMIC without the addition of any cations).

Without the addition of Zn^{2+}, the quantum yields of the two molecules are smaller than 0.002 (using quinine sulfate[30] as the standard at r.t. in most of the tested solvents except ethanol). The addition of a saturated solution of Zn^{2+} (1 mM) resulted in greatly enhanced quantum yields of 0.04 for OPMIC and 0.07 for Boc-OPMIC in acetone (Figure 1). The emission maximum of Zn^{2+}-loaded OPMIC was at 441 nm and that of Boc-OPMIC was at 432 nm (Table 1). Similar results were observed in other organic solvents including acetonitrile, tetrahydrofuran (THF), and dioxane (Figure S3). Zn^{2+}-loaded OPMIC showed the highest quantum yield of 0.055 in THF. Conversely, the quantum yield is only 0.012 in acetonitrile, a quarter of that in THF. For Zn^{2+}-loaded Boc-OPMIC, quantum yields of around 0.07 were observed in all the solvents.

Table 1. The excitation (λ_{Ex}), emission (λ_{Em}), and absorbance wavelengths (λ_{Abs}) [nm] of OPMIC and Boc-OPMIC with (+) and without (–) Zn^{2+}.

	Solvent	Zn^{2+}	λ_{Ex}[a]	λ_{Em}[a]	λ_{Abs}[b]
OPMIC	acetone	–			384 (*), 398 (s)
		+	364	441	358 (*), 374 (s)
	THF	–			259, 386 (*), 397 (s)
		+	364	442	256, 361 (*), 375 (s)
	CH_3CN	–			259, 382 (*), 396 (s)
		+	391	458	259, 370 (*), 383 (s)
	ethanol	–	368	433	308, 377 (*), 395 (s)
		+	365	434	258, 370 (*)
	dioxane	–			261, 384 (*), 403
		+	362	434	258, 361 (*), 380 (s)
Boc-OPMIC	acetone	–			369 (*), 388 (s)
		+	355	431	360 (*), 375 (s)
	THF	–			261, 371 (*), 388 (s)
		+	356	432	259, 366 (*)
	CH_3CN	–			263, 369 (*), 388 (s)
		+	356	430	263, 362 (*), 380 (s)
	ethanol	–	369	431	264, 367 (*), 385 (s)
		+	363	431	264, 367 (*), 385 (s)
	dioxane	–			261, 371 (*), 392 (s)
		+	357	425	260, 364 (*), 386 (s)

[a] Data at room temp. The values for Zn^{2+}-free solutions were less reliable and are not shown here, except those in ethanol. [b] *: the highest peak; s: shoulder peak.

The Zn^{2+} binding to both molecules was reversible. The enhancement of fluorescence of OPMIC and Boc-OPMIC as a function of Zn^{2+} in dioxane fitted well with Hill's equation with Hill coefficients of 0.9 and 1.3 for OPMIC and Boc-OPMIC, respectively, which suggests that both molecules bind to Zn^{2+} in a 1:1 ratio.[31] The resulting dissociation constants are 10 ± 1 μM for OPMIC and 60 ± 5 μM for Boc-OPMIC. In more volatile organic solvents, estimated Zn^{2+} binding affinities from titrations were similar to those obtained in dioxane (Figure S4).

The results suggested that the Boc-group did not alter the Zn^{2+} binding mode significantly but influenced the fluorescence in three ways: (1) it shifted the emission maxima of the molecules. The Boc group blueshifted the emission by about 10 nm in acetone and THF and by about 28 nm in acetonitrile (Table 1). The methyl groups in Boc might contribute to this shift by providing a more hydrophobic environment for the chromophore; (2) the Boc group enhanced the quantum yields of the Zn^{2+}-loaded molecule. In acetonitrile, the fluorescence intensity of Boc-OPMIC was more than five times that of OPMIC; (3) the Boc group lowered the Zn^{2+} binding affinity.

Relationship between Fluorescence and Bond Rotation

To reveal the mechanism of Zn^{2+}-induced fluorescence, the structure of Boc-OPMIC was investigated by X-ray crystallography and theoretical calculations. The crystal structure of Zn^{2+}-free Boc-OPMIC (Figure 3) contains two forms, with the donor atoms in *cis* and *trans* configurations. This explains the controversial effects of the Boc-group on the Zn^{2+}-binding affinity and fluorescence intensity. First, a conformation transition is necessary to convert the molecule from the Zn^{2+}-free to the Zn^{2+}-loaded state as shown inset in Figure 1. The steric hindrance introduced by the Boc group produces a higher energy barrier for this transition, which leads to a lower Zn^{2+}-binding affinity. On the other hand, once the molecule is in the Zn^{2+}-loaded state, this energy barrier also prevents the aryl–alkene bond rotation in Zn^{2+}-loaded molecules. As the prevention of this aryl–alkene bond rotation is key for the emission, the presence of the Boc group resulted in enhanced fluorescence.

DFT and time-dependent (TD)-DFT calculations[32,33] agreed with the crystallographic study that the configuration with two ligand nitrogen atoms on opposite sides possessed a lower energy level for Zn^{2+}-free OPMIC. In addition, the enhanced oscillator strength indicated increased fluorescence with Zn^{2+} binding (Table 2).

Table 2. The TD-DFT predicted emission wavelengths of OPMIC in acetone, acetonitrile, and ethanol with (+) and without (–) Zn^{2+}.

Solvent	Zn^{2+}	λ_{Em} [nm]	Excitation energy [eV]	f[a]	Weight of L→H transition
Acetone	–	441.4	2.81	1.12	0.7
	+	428.6	2.89	1.15	0.7
Ethanol	–	442.3	2.80	1.13	0.7
	+	429.5	2.89	1.16	0.7
Acetonitrile	–	443.6	2.79	1.13	0.7
	+	430.9	2.88	1.16	0.7

[a] Oscillator strength.

The fluorescence of the molecules was measured at low temperature. Because of the different melting temperatures (–114, –95, –108, and –45 °C for ethanol, acetone, THF, and acetonitrile, respectively), low-temperature fluorescence in different solvents cannot be quantitatively compared but it is helpful to understand the fluorescence mechanism qualitatively. At low temperature, the fluorescence emission was greatly enhanced both with and without Zn^{2+} in all solvents compared to that at r.t. In acetone and THF, quantum yields close to 0.3 were obtained for Zn^{2+}-free OPMIC, which is two orders of magnitude higher than that at r.t. For Zn^{2+}-loaded OPMIC, depending on the solvent, the quantum yields were enhanced several fold to 0.25–0.3. These results show that the inhibition of the bond rotation, in other words, prevention of the radiationless relaxation of the excited molecules through thermodynamic pathways, is the key for fluorescence.

In addition, fine structure was observed in each spectrum at low temperature. Two major peaks with several shoulders were observed for Zn^{2+}-free OPMIC (Figure 4). The major peaks suggested that multiple configurations coexist, which agree with the crystallographic and theoretical studies. The emission wavelengths at ca. 442 nm match the predictions from TD-DFT calculations. The shoulders likely arose from different orbital vibrations. Similar results were obtained for Zn^{2+}-loaded OPMIC (the broad peak obtained in acetone and THF is likely to be the combination of two close emissions). The results suggest that Zn^{2+}-OPMIC also possesses more than one configuration but the detailed structures are yet to be revealed. For Boc-OPMIC, one more major peak was observed both with and without Zn^{2+}, which indicates that the Boc group also has more than one configuration in the molecule.

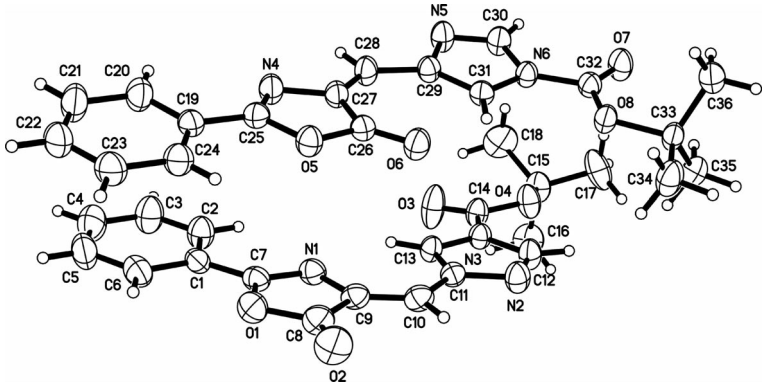

Figure 3. The crystal structure of Boc-OPMIC. The crystal was a red needle, which was formed from an ethyl acetate/petroleum ether (4:1) solution of Boc-OPMIC at r.t.

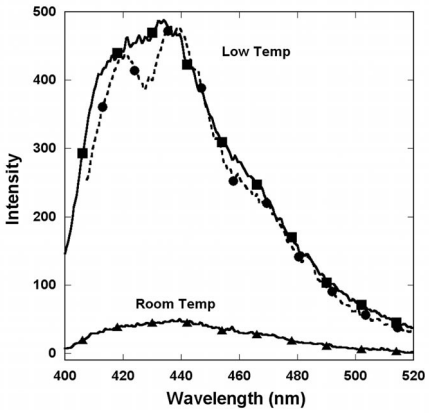

Figure 4. The emissions of OPMIC (20 μM) at low temperature in acetone with (solid) and without (dashed) Zn^{2+} compared to Zn^{2+}-loaded OPMIC at r.t.

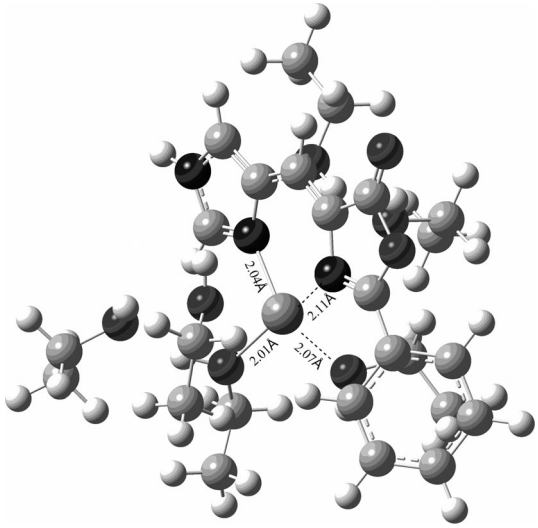

Figure 5. The TD-DFT predicted Zn^{2+} binding mode of OPMIC in ethanol. Two ethanol molecules chelate Zn^{2+} together with OPMIC. The distances of the ethanol oxygen atoms to the Zn^{2+} are 2.01 and 2.07 Å, respectively. Red: oxygen; blue: nitrogen; gray: carbon; purple: zinc; small balls: hydrogen.

Solvent Effects

The DFT and TD-DFT calculations suggested that the Zn^{2+} binding would blueshift the emission wavelengths of the molecules (Table 2). Consistent with this, Zn^{2+} binding slightly blueshifted the emission of OPMIC in acetone and THF by 3–4 nm. However, it is noteworthy that significant redshifts (15 and 23 nm for OPMIC and Boc-OPMIC, respectively) were observed on addition of Zn^{2+} in acetonitrile (Figure S6). This was due to direct interaction between the solvent molecules and the fluorophore system, which was not included in the calculation. Typically, a cation-induced emission wavelength shift indicates a photo-induced charge transfer between the ionophore and fluorophore for normal sensors.[1] In OPMIC, the same groups functioned as both ionophore and fluorophore. Therefore, we believe that the Zn^{2+}-induced redshift in acetonitrile indicates intermolecular charge transfer.

The chelation of a Zn^{2+} ion requires four ligand donor atoms,[34] of which OPMIC provides two. The other two donors are provided by the solvent. The nitrogen atom of acetonitrile could function as an electron donor when it chelates Zn^{2+} together with OPMIC. As a result, an intermolecular charge transfer occurred through the bound Zn^{2+} when the molecule was excited. This indeed enlarged the π-conjugated system that led to redshifts of the excitation and emission wavelengths. Further theoretical simulation with M06–2X/6-31g* supported this hypothesis. When solvent molecules were placed close to the Zn^{2+}, the nitrogen atom of the acetonitrile or the oxygen atom of the ethanol could be involved in the Zn^{2+} binding together with OPMIC (Figure 5). The predicted distances of 2.01 and 2.07 Å are close to the measured ethanol O–Zn^{2+} distances of 1.90 and 1.98 Å in a Fe–ZnO nanoparticle that senses ethanol.[35]

Furthermore, Zn^{2+}-free OPMIC possesses more intense fluorescence signals in ethanol than in other solvents. Alcohols could form weak hydrogen bonds with aromatic rings.[36] The TD-DFT calculation suggested that ethanol molecules directly interact with OPMIC. Although this interaction is not as powerful as that of Zn^{2+} binding, the steric hindrance it introduces enhances fluorescence. When Zn^{2+} was added, the ethanol molecule was replaced.

The UV/Vis absorbance of Zn^{2+}-free OPMIC at 308 nm in ethanol supported the results of the calculations. As observed in other solvents, the absorbance for the benzene ring in OPMIC was at 260 nm. The fact that this absorbance was missing suggested that the π-conjugated system of the benzene ring was altered, which could be caused by the interaction of ethanol with the ring. The Zn^{2+} binding interrupted this interaction and shifted the absorbance back to 260 nm.

Conclusions

In conclusion, a GFP-like fluorescent Zn^{2+} sensor OPMIC was designed and synthesized. The molecule presented Zn^{2+}-related fluorescence in organic solvents. The binding of Zn^{2+} to the imidazole and oxole rings in OPMIC inhibited the free rotation of the aryl–alkene bond that links the two rings, which led the excited molecules to relax through the emission pathway instead of the thermodynamic pathway. The experimental and theoretical results showed that the solvents affected the emissions by direct or indirect interaction with the molecules. The study demonstrated that GFP-like chromophores have the potential to be applied without the protein context.

Experimental Section

The synthesis of Boc-OPMIC and OPMIC was performed as shown in Scheme 1.

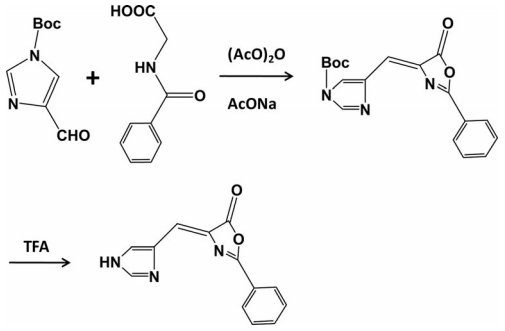

Scheme 1. The Synthesis of Boc-OPMIC and OPMIC.

Synthesis of Imidazole-4-carboxaldehyde: To a stirred mixture of imidazole-4-carboxaldehyde (0.475 g, 5 mmol), 4-(dimethylamino)-pyridine (0.06 g, 0.6 mmol) and acetonitrile (5 mL) was added an acetonitrile solution (5 mL) of di-*tert*-butyl dicarbonate (1.31 g) dropwise. The resulting mixture was stirred at r.t. for 3 h. Colorless crystals were obtained after removing the solvent under reduced pressure, and the product was further purified by column chromatography (diethyl ether/ethyl acetoacetate 3:1).

Synthesis of Boc-OPMIC: To a mixture of Boc-protected imidazole-4-carboxaldehyde (0.974 g, 4.97 mmol), 2-benzamidoacetic acid (0.969 g, 5.36 mmol), and anhydrous sodium acetate (0.414 g, 5 mmol) was added acetic anhydride (4 mL). As the temperature was increased, the solid gradually melted, and a color change to deep yellow was observed. The mixture was stirred for a further 80 min at 75 °C. The mixture was concentrated in vacuo, and the crude product purified by column chromatography (diethyl ether/ethyl acetoacetate: 4:1) to give Boc-OPMIC.

Synthesis of OPMIC: Boc-OPMIC (0.2 g, 0.59 mmol) was dissolved in TFA (0.919 mL) at 0 °C and the solution was kept at r.t. for 1 h (the yellow solution turned deep yellow in color). The TFA was evaporated under reduced pressure and the residue was kept in vacuo for 1 h to remove residual TFA. The residue was partitioned between CH_2Cl_2 and water, using NaOH (1 M) to adjust the pH to 10–11. The chloroform layer was dried and evaporated under reduced pressure to leave a yellow powder.

Theoretical Calculations: Theoretical studies by DFT and TD-DFT were performed to investigate the structure and fluorescent properties of OPMIC in three organic solvents (acetone, acetonitrile, and ethanol) with the polarizable continuum model as the solvent model. M06-2X/6-31g* and TD M06-2X/6-31g* methods were utilized for geometry optimization of the molecules at ground and excited states, respectively. On the basis of the geometric structures of the excited states in the solvents, the corresponding emission wavelengths were obtained. The emission wavelengths with the largest oscillator strength were ascribed to the S1→S0 transition. All emissions are assigned as having π→π* character arising from S1, the highest occupied molecular orbital to the lowest unoccupied molecular orbital transition. The other transitions are not included here.

Fluorescence Measurements: The fluorescence spectra were collected with dye concentrations of about 20 μM in various solvents at r.t. and low temperature. The excitation wavelengths varied in the different solvents [356, 363, 356, 355, and 357 nm for Boc-OPMIC and 391, 365, 364, 364, and 362 nm for OPMIC in acetonitrile, ethanol, acetone, THF, and dioxane, respectively]. For titration in dioxane, the excitation wavelength was fixed at 357 nm for Boc-OPMIC and 362 nm for OPMIC. The cation concentrations were all 1 mM for the selectivity study. For the titration, Zn^{2+} stock solutions of 2 and 20 mM in the dye solution in dioxane were used for the low and high Zn^{2+} points, respectively. For low temperature fluorescence spectra, the dyes in different solvents were quickly frozen in dry ice/methanol. Then the samples were placed at r.t. to melt. Data collection was initiated immediately after the frozen samples had completely melted and was finished in 1–2 min so that the emission spectra were obtained at temperatures close to the melting points of the solvents used (–114, –95, –108, and –45 °C for ethanol, acetone, THF, and acetonitrile, respectively).

Supporting Information (see footnote on the first page of this article): NMR, UV/Vis, and more fluorescence data at r.t. and low temperature.

Acknowledgments

We thank the National Natural Science Foundation of China (NSFC), grant number 30870491 (to W. Y.) for financially supporting this work.

[1] P. J. Jiang, Z. J. Guo, *Coord. Chem. Rev.* **2004**, *248*, 205.
[2] K. Sarkar, K. Dhara, M. Nandi, P. Roy, A. Bhaumik, P. Banerjee, *Adv. Funct. Mater.* **2009**, *19*, 223.
[3] S. Aoki, K. Sakurama, R. Ohshima, N. Matsuo, Y. Yamada, R. Takasawa, S. I. Tanuma, K. Talkeda, E. Kimura, *Inorg. Chem.* **2008**, *47*, 2747.
[4] G. K. Andrews, *Biometals* **2001**, *14*, 223.
[5] J. E. Coleman, *Curr. Opin. Chem. Biol.* **1998**, *2*, 222.
[6] A. Q. Truong-Tran, J. Carter, R. E. Ruffin, P. D. Zalewski, *Biometals* **2001**, *14*, 315.
[7] M. F. Langelier, K. M. Servent, E. E. Rogers, J. M. Pascal, *J. Biol. Chem.* **2008**, *283*, 4105.
[8] D. Buccella, J. A. Horowitz, S. J. Lippard, *J. Am. Chem. Soc.* **2011**, *133*, 4101.
[9] A. I. Bush, R. E. Tanzi, *Proc. Natl. Acad. Sci. USA* **2002**, *99*, 7317.
[10] M. P. Cuajungco, G. J. Lees, *Neurobiol. Dis.* **1997**, *4*, 137.
[11] E. Kimura, T. Koike, *Chem. Soc. Rev.* **1998**, *27*, 179.
[12] E. Kimura, S. Aoki, *Biometals* **2001**, *14*, 191.
[13] W. Huang, Y. N. Li, Q. Liu, H. L. Wu, Y. Q. Li, *Chin. J. Anal. Chem.* **2009**, *37*, 1142.
[14] N. C. Shaner, G. H. Patterson, M. W. Davidson, *J. Cell Sci.* **2007**, *120*, 4247.
[15] R. Y. Tsien, *Annu. Rev. Biochem.* **1998**, *67*, 509.
[16] D. P. Barondeau, C. J. Kassmann, J. A. Tainer, E. D. Getzoff, *J. Am. Chem. Soc.* **2002**, *124*, 3522.
[17] X. He, A. F. Bell, P. J. Tonge, *Org. Lett.* **2002**, *4*, 1523.
[18] S. Kojima, H. Ohkawa, T. Hirano, S. Maki, H. Niwa, M. Ohashi, S. Inouye, F. I. Tsuji, *Tetrahedron Lett.* **1998**, *39*, 5239.
[19] L. Wu, K. Burgess, *J. Am. Chem. Soc.* **2008**, *130*, 4089.
[20] I. V. Yampolsky, A. A. Kislukhin, T. T. Amatov, D. Shcherbo, V. K. Potapov, S. Lukyanov, K. A. Lukyanov, *Bioorg. Chem.* **2008**, *36*, 96.
[21] M. Zimmer, *Chem. Rev.* **2002**, *102*, 759.
[22] M. Ormo, A. B. Cubitt, K. Kallio, L. A. Gross, R. Y. Tsien, S. J. Remington, *Science* **1996**, *273*, 1392.
[23] F. Yang, L. G. Moss, G. N. Phillips Jr., *Nat. Biotechnol.* **1996**, *14*, 1246.
[24] J. Dong, K. M. Solntsev, L. M. Tolbert, *J. Am. Chem. Soc.* **2006**, *128*, 12038.
[25] A. Follenius-Wund, M. Bourotte, M. Schmitt, F. Iyice, H. Lami, J. J. Bourguignon, J. Haiech, C. Pigault, *Biophys. J.* **2003**, *85*, 1839.
[26] J. T. Kang, G. Y. Zhao, J. W. Xu, W. Yang, *Chem. Commun.* **2010**, *46*, 2868.
[27] M. A. Filatov, A. Y. Lebedev, S. N. Mukhin, S. A. Vinogradov, A. V. Cheprakov, *J. Am. Chem. Soc.* **2010**, *132*, 9552.

[28] A. Baldridge, K. M. Solntsev, C. Song, T. Tanioka, J. Kowalik, K. Hardcastle, L. M. Tolbert, *Chem. Commun.* **2010**, *46*, 5686.
[29] Y. Li, L. Shi, L. X. Qin, L. L. Qu, C. Jing, M. B. Lan, T. D. James, Y. T. Long, *Chem. Commun.* **2011**, *47*, 4361.
[30] D. F. Eaton, *J. Photochem. Photobiol. B* **1988**, *2*, 523.
[31] S. Forsen, S. Linse, *Trends Biochem. Sci.* **1995**, *20*, 495.
[32] M. J. Frisch, G. W. Trucks, H. B. Schlegel, G. E. Scuseria, M. A. Robb, J. R. Cheeseman, G. Scalmani, V. Barone, B. Mennucci, G. A. Petersson, H. Nakatsuji, M. Caricato, X. Li, H. P. Hratchian, A. F. Izmaylov, J. Bloino, G. Zheng, J. L. Sonnenberg, M. Hada, M. Ehara, K. Toyota, R. Fukuda, J. Hasegawa, M. Ishida, T. Nakajima, Y. Honda, O. Kitao, H. Nakai, T. Vreven, J. J. A. Montgomery, J. E. Peralta, F. Ogliaro, M. Bearpark, J. J. Heyd, E. Brothers, K. N. Kudin, V. N. Staroverov, R. Kobayashi, J. Normand, K. Raghavachari, A. Rendell, J. C. Burant, S. S. Iyengar, J. Tomasi, M. Cossi, N. Rega, J. M. Millam, M. Klene, J. E. Knox, J. B. Cross, V. Bakken, C. Adamo, J. Jaramillo, R. Gomperts, R. E. Stratmann, O. Yazyev, A. J. Austin, R. Cammi, C. Pomelli, J. W. Ochterski, R. L. Martin, K. Morokuma, V. G. Zakrzewski, G. A. Voth, P. Salvador, J. J. Dannenberg, S. Dapprich, A. D. Daniels, O. Farkas, J. B. Foresman, J. V. Ortiz, J. Cioslowski, J. Fox, *Gaussian 09*, Revision A.01, Gaussian, Inc., Wallingford, CT, **2009**.
[33] D. Jacquemin, E. A. Perpete, I. Ciofini, C. Adamo, R. Valero, Y. Zhao, D. G. Truhlar, *J. Chem. Theory Comput.* **2010**, *6*, 2071.
[34] L. Rulisek, J. Vondrasek, *J. Inorg. Biochem.* **1998**, *71*, 115.
[35] G.-H. Kuo, H. Paul Wang, H. H. Hsu, J. Wang, Y. M. Chiu, C.-J. G. Jou, T. F. Hsu, F.-L. Chen, *J. Nanomater.* **2009**, DOI: 10.1155/2009/316035.
[36] R. L. Brinkley, R. B. Gupta, *Aiche J.* **2001**, *47*, 948.

Received: June 17, 2011
Published Online: October 24, 2011

